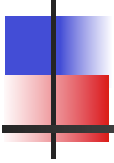
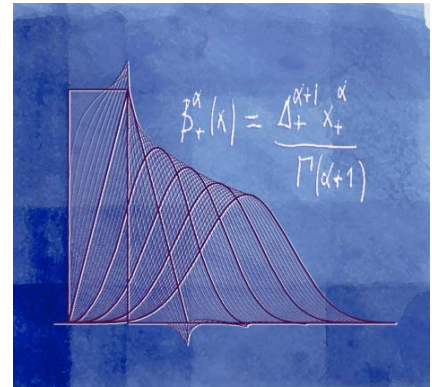


Sparse modeling and the resolution of inverse problems in biomedical imaging



Michael Unser
Biomedical Imaging Group
EPFL, Lausanne, Switzerland

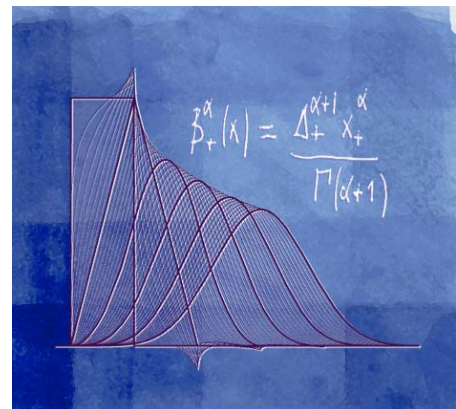


Plenary talk, *IEEE Int. Symp. Biomedical Imaging (ISBI'15)*, 16-19 April, 2015, New York, USA

IEEE International Symposium on Biomedical Imaging: Macro to Nano

7-10 July 2002

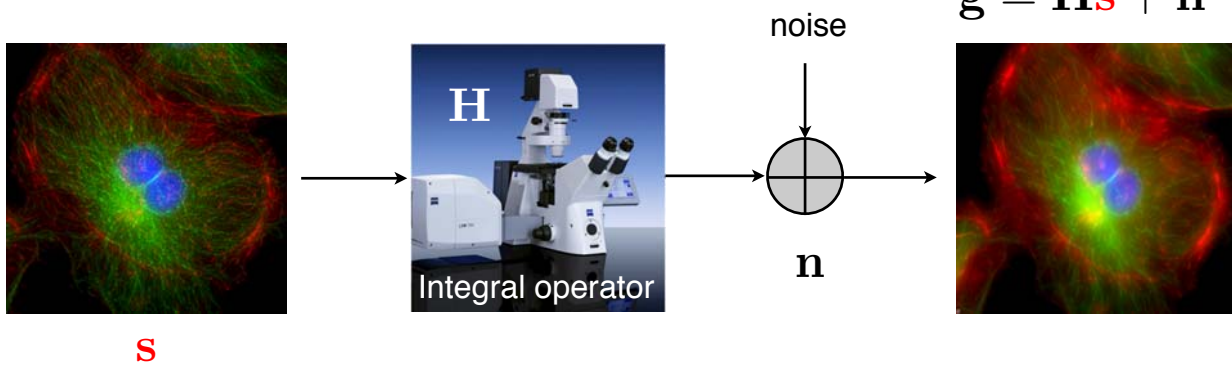
Washington, DC, USA



Logo design: Annette Unser

Variational formulation of image reconstruction

Linear forward model



Ill-posed inverse problem: recover \mathbf{s} from noisy measurements \mathbf{g}

Reconstruction as an optimization problem

$$\mathbf{s}^* = \operatorname{argmin} \underbrace{\|\mathbf{g} - \mathbf{H}\mathbf{s}\|_2^2}_{\text{data consistency}} + \underbrace{\lambda \mathcal{R}(\mathbf{s})}_{\text{regularization}}$$

3

Classical reconstruction = linear algorithm

$$\mathbf{s}^* = \operatorname{argmin} \underbrace{\|\mathbf{g} - \mathbf{H}\mathbf{s}\|_2^2}_{\text{data consistency}} + \underbrace{\lambda \mathcal{R}(\mathbf{s})}_{\text{regularization}}$$

Quadratic regularization (Tikhonov)

$$\mathcal{R}(\mathbf{s}) = \|\mathbf{L}\mathbf{s}\|^2$$

$$\text{Formal linear solution: } \mathbf{s} = (\mathbf{H}^T \mathbf{H} + \lambda \mathbf{L}^T \mathbf{L})^{-1} \mathbf{H}^T \mathbf{g} = \mathbf{R}_\lambda \cdot \mathbf{g}$$

$$\Updownarrow \quad \mathbf{L} = \mathbf{C}_s^{-1/2}: \text{Whitening filter}$$

Statistical formulation under Gaussian hypothesis

Wiener (LMMSE) solution = Gauss MMSE = Gauss MAP

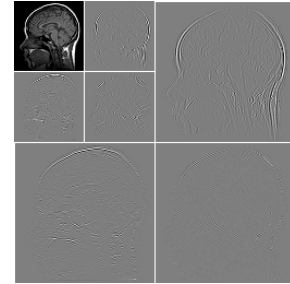
$$\mathbf{s}_{\text{MAP}} = \operatorname{argmin}_{\mathbf{s}} \underbrace{\frac{1}{\sigma^2} \|\mathbf{g} - \mathbf{H}\mathbf{s}\|_2^2}_{\text{Data Log likelihood}} + \underbrace{\|\mathbf{C}_s^{-1/2} \mathbf{s}\|_2^2}_{\text{Gaussian prior likelihood}}$$

$$\text{Signal covariance: } \mathbf{C}_s = \mathbb{E}\{\mathbf{s} \cdot \mathbf{s}^T\}$$

4

Current trend: non-linear algorithms (l_1 optimization)

$$\mathbf{s}^* = \underset{\mathbf{s}}{\operatorname{argmin}} \underbrace{\|\mathbf{y} - \mathbf{H}\mathbf{s}\|_2^2}_{\text{data consistency}} + \underbrace{\lambda \mathcal{R}(\mathbf{s})}_{\text{regularization}}$$



■ Wavelet-domain regularization

Wavelet expansion: $\mathbf{s} = \mathbf{W}\mathbf{v}$ (typically, sparse)

Wavelet-domain sparsity-constraint: $\mathcal{R}(\mathbf{s}) = \|\mathbf{v}\|_{\ell_1}$ with $\mathbf{v} = \mathbf{W}^{-1}\mathbf{s}$

(Nowak et al., Daubechies et al. 2004)

■ ℓ_1 regularization (Total variation=TV) (Rudin-Osher, 1992)

$\mathcal{R}(\mathbf{s}) = \|\mathbf{L}\mathbf{s}\|_{\ell_1}$ with \mathbf{L} : gradient

■ Compressed sensing/sampling (Candes-Romberg-Tao; Donoho, 2006)

5

Key research questions (for biomedical imaging)

① Formulation of ill-posed reconstruction problem

*Statistical modeling (beyond Gaussian)
supporting **non-linear reconstruction** schemes
(including CS)*

Sparse stochastic processes

② Efficient implementation for large-scale imaging problem

ADMM = smart chaining of simple modules

③ Future trends and open issues

6

OUTLINE

- Variational formulation of inverse problems ✓
- **Statistical modeling**
Introduction to sparse stochastic processes
 - Generalized innovation model
 - Statistical characterization of signal
- **Algorithm design**
Reconstruction of biomedical images
 - Discretization of inverse problem
 - Generic MAP estimator (iterative reconstruction algorithm)
 - Applications



Deconvolution microscopy
Computed tomography
Cryo-electron tomography
Differential phase-contrast tomography

7

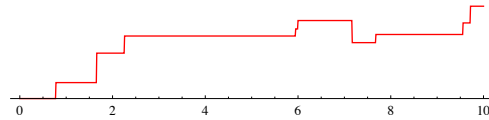
A decorative graphic consisting of a grid of colored squares in various shades of blue, teal, and green, arranged in a pattern that resembles a stylized letter 'A' or a similar shape.

An
introduction
to sparse
stochastic
processes

8

Random spline: archetype of sparse signal

non-uniform spline of degree 0



$$Ds(t) = \sum_n a_n \delta(t - t_n) = w(t)$$

Random weights $\{a_n\}$ i.i.d. and random knots $\{t_n\}$ (Poisson with rate λ)

■ Anti-derivative operators

Shift-invariant solution: $D^{-1}\varphi(t) = (\mathbb{1}_+ * \varphi)(t) = \int_{-\infty}^t \varphi(\tau) d\tau$

Scale-invariant solution: $D_0^{-1}\varphi(t) = \int_0^t \varphi(\tau) d\tau$

9

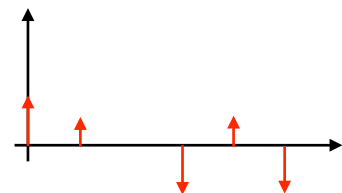
Compound Poisson process

■ Stochastic differential equation

$$Ds(t) = w(t)$$

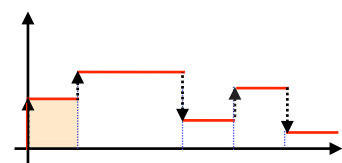
with boundary condition $s(0) = 0$

Innovation: $w(t) = \sum_n a_n \delta(t - t_n)$



■ Formal solution

$$\begin{aligned} s(t) &= D^{-1}w(t) = \sum_n a_n D^{-1}\{\delta(\cdot - t_n)\}(t) \\ &= \sum_n a_n \mathbb{1}_+(t - t_n) \end{aligned}$$

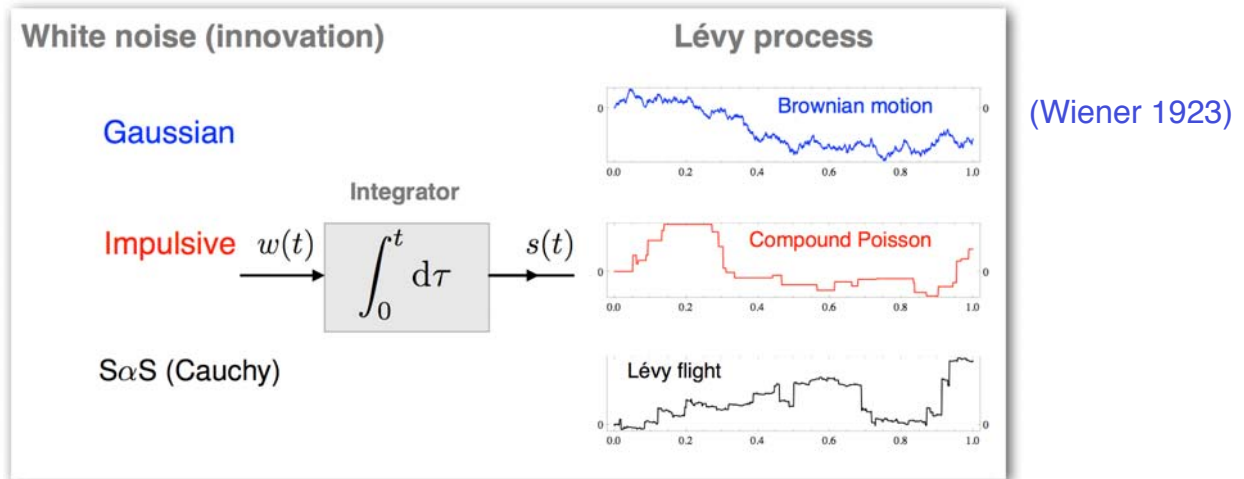


10

Lévy processes: all admissible brands of innovations

Generalized innovations : white Lévy noise with $\mathbb{E}\{w(t)w(t')\} = \sigma_w^2 \delta(t - t')$

$$Ds = w \quad (\text{perfect decoupling!})$$



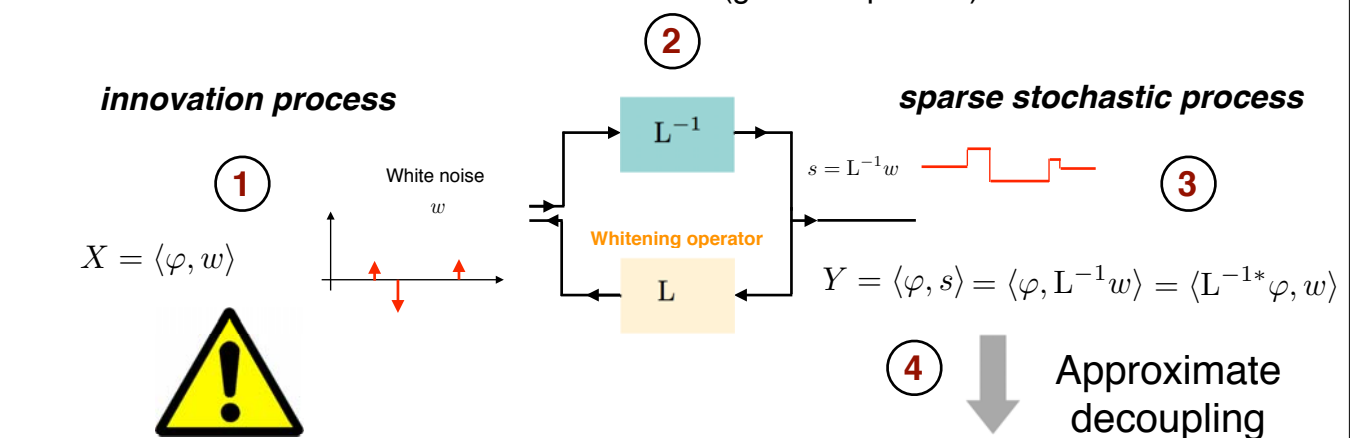
(Paul Lévy circa 1930)

Generalized innovation model

Theoretical framework: Gelfand's theory of generalized stochastic processes

Generic test function $\varphi \in \mathcal{S}$ plays the role of index variable

Solution of SDE (general operator)



Proper definition of **continuous-domain** white noise

(Unser et al, IEEE-IT 2014)

Regularization operator vs. wavelet analysis

Main feature: inherent sparsity
(few significant coefficients)

Infinite divisibility and Lévy exponents

Definition: A random variable X with generic pdf $p_{\text{id}}(x)$ is **infinitely divisible** (id) iff., for any $N \in \mathbb{Z}^+$, there exist i.i.d. random variables X_1, \dots, X_N such that $X \stackrel{d}{=} X_1 + \dots + X_N$.

■ Rectangular test function

$$\begin{aligned}
 X = \langle w, \text{rect} \rangle &= \langle \text{blue noise}, \text{rect of width 1} \rangle \\
 &= \langle \text{blue noise}, \text{rect of width } \frac{1}{n} \rangle + \dots + \langle \text{blue noise}, \text{rect of width } \frac{1}{n} \rangle
 \end{aligned}$$

i.i.d.

Proposition

The random variable $X = \langle w, \text{rect} \rangle$ where w is a generalized innovation process is infinitely divisible. It is uniquely characterized by its **Lévy exponent** $f(\omega) = \log \hat{p}_{\text{id}}(\omega)$.

$$\hat{p}_{\text{id}}(\omega) = e^{f(\omega)} = \int_{\mathbb{R}} p_{\text{id}}(x) e^{j\omega x} dx$$

Bottom line: There is a one-to-one correspondence between Lévy exponents and infinitely divisible distributions and, by extension, innovation processes.

13

Probability laws of innovations are infinite divisible

$$\begin{aligned}
 X = \langle w, \varphi \rangle &= \langle \text{blue noise}, \text{smooth curve } \varphi \rangle \triangleq \lim_{n \rightarrow \infty} \langle \text{blue noise}, \text{step function } \varphi_n \rangle \\
 &= \lim_{n \rightarrow \infty} \langle \text{blue noise}, \text{rect of width } \frac{1}{n} \rangle + \dots + \langle \text{blue noise}, \text{rect of width } \frac{1}{n} \rangle
 \end{aligned}$$

■ Statistical description of white Lévy noise w (innovation)

- Characterized by canonical (p -admissible) Lévy exponent $f(\omega)$
- Generic observation: $X = \langle \varphi, w \rangle$ with $\varphi \in L_p(\mathbb{R}^d)$
- X is **infinitely divisible** with (modified) Lévy exponent

$$f_{\varphi}(\omega) = \log \hat{p}_X(\omega) = \int_{\mathbb{R}^d} f(\omega \varphi(x)) dx$$

14

⇒ Probability laws of sparse processes are id

■ Analysis: go back to **innovation process**: $w = Ls$

■ Generic random observation: $X = \langle \varphi, w \rangle$ with $\varphi \in \mathcal{S}(\mathbb{R}^d)$ or $\varphi \in L_p(\mathbb{R}^d)$ (by extension)

■ Linear functional: $Y = \langle \psi, s \rangle = \langle \psi, L^{-1}w \rangle = \langle \underbrace{L^{-1*}\psi}_\phi, w \rangle$

If $\phi = L^{-1*}\psi \in L_p(\mathbb{R}^d)$ then $Y = \langle \psi, s \rangle = \langle \phi, w \rangle$ is **infinitely divisible** with Lévy exponent $f_\phi(\omega) = \int_{\mathbb{R}^d} f(\omega\phi(x)) dx$

$$\Rightarrow p_Y(y) = \mathcal{F}^{-1}\{e^{f_\phi(\omega)}\}(y) = \int_{\mathbb{R}} e^{f_\phi(\omega) - j\omega y} \frac{d\omega}{2\pi}$$

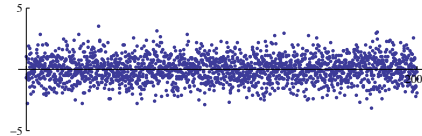
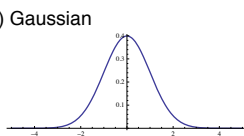


= explicit form of pdf

Examples of infinitely divisible laws

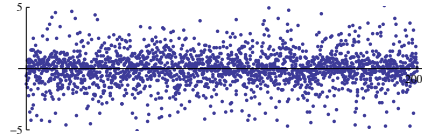
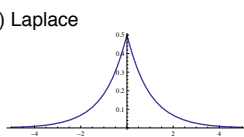
$p_{id}(x)$

(a) Gaussian



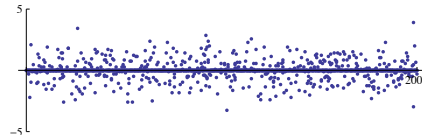
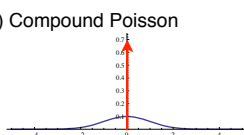
$$p_{\text{Gauss}}(x) = \frac{1}{\sqrt{2\pi\sigma^2}} e^{-\frac{x^2}{2\sigma^2}}$$

(b) Laplace



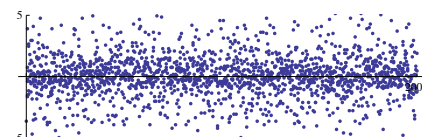
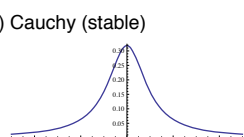
$$p_{\text{Laplace}}(x) = \frac{\lambda}{2} e^{-\lambda|x|}$$

(c) Compound Poisson



$$p_{\text{Poisson}}(x) = \mathcal{F}^{-1}\{e^{\lambda(\hat{p}_A(\omega)-1)}\}$$

(d) Cauchy (stable)



$$p_{\text{Cauchy}}(x) = \frac{1}{\pi(x^2 + 1)}$$

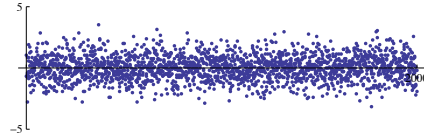
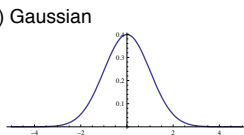
Sparsier

Characteristic function: $\hat{p}_{id}(\omega) = \int_{\mathbb{R}} p_{id}(x) e^{j\omega x} dx = e^{f(\omega)}$

Examples of id noise distributions

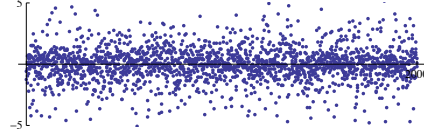
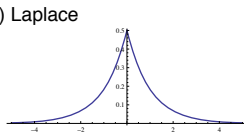
$p_{id}(x)$ Observations: $X_n = \langle w, \text{rect}(\cdot - n) \rangle$

(a) Gaussian



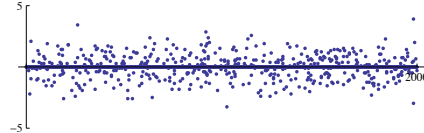
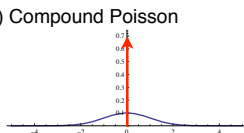
$$f(\omega) = -\frac{\sigma_0^2}{2} |\omega|^2$$

(b) Laplace



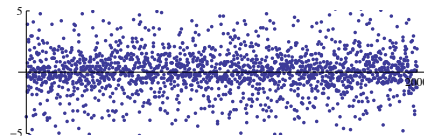
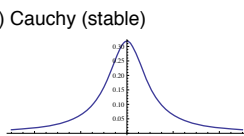
$$f(\omega) = \log\left(\frac{1}{1+\omega^2}\right)$$

(c) Compound Poisson



$$f(\omega) = \lambda \int_{\mathbb{R}} (e^{jx\omega} - 1) p(x) dx$$

(d) Cauchy (stable)



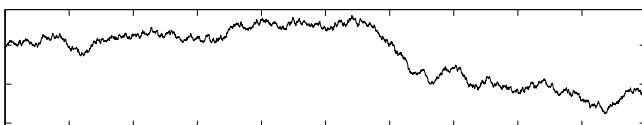
$$f(\omega) = -s_0 |\omega|$$

Sparsier

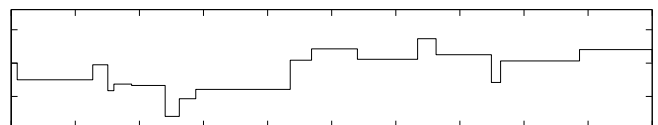
Complete mathematical characterization: $\widehat{\mathcal{P}}_w(\varphi) = \exp\left(\int_{\mathbb{R}^d} f(\varphi(x)) dx\right)$

Generation of self-similar processes: $s = L^{-1}w$

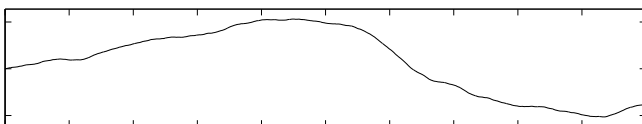
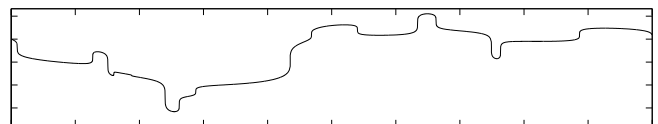
$$L \xleftrightarrow{\mathcal{F}} (j\omega)^{H+\frac{1}{2}} \Rightarrow L^{-1}: \text{fractional integrator}$$



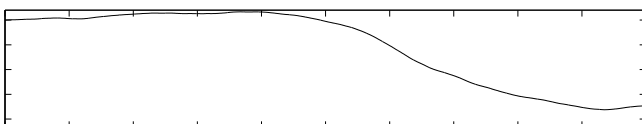
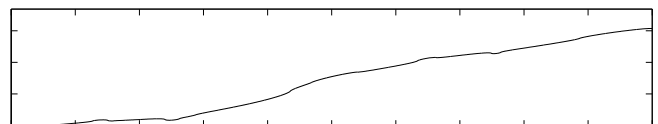
H=0.5



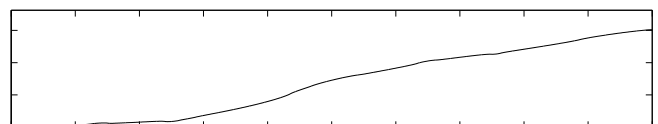
H=0.75



H=1.25



H=1.5



Gaussian

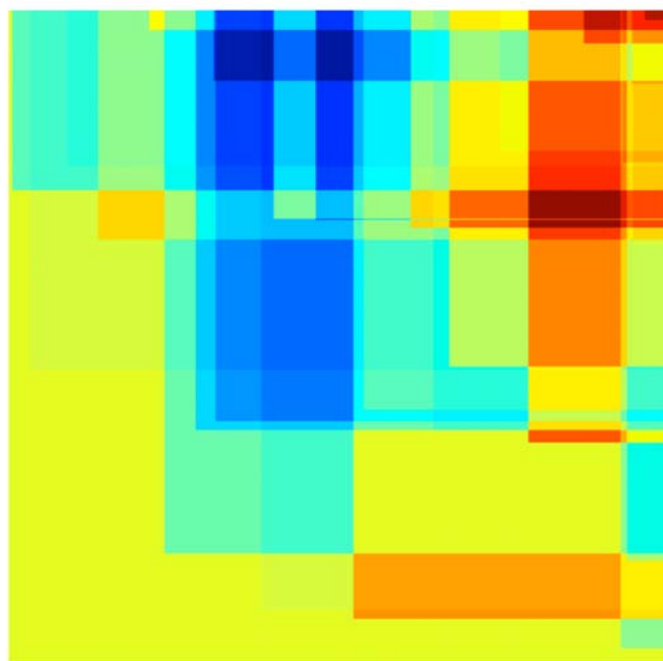
Sparse (generalized Poisson)

Fractional Brownian motion (Mandelbrot, 1968)

(U.-Tafti, IEEE-SP 2010)

Aesthetic sparse signal: the Mondrian process

$$L = D_x D_y \xleftrightarrow{\mathcal{F}} (j\omega_x)(j\omega_y)$$



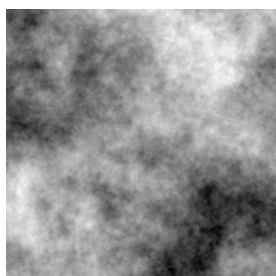
$$\lambda = 30$$

19

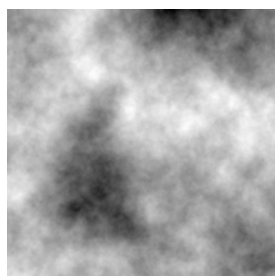
Scale- and rotation-invariant processes

Stochastic partial differential equation : $(-\Delta)^{\frac{H+1}{2}} s(\mathbf{x}) = w(\mathbf{x})$

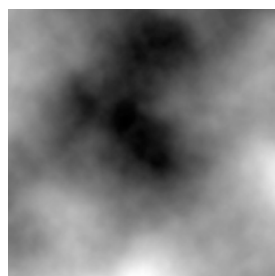
Gaussian



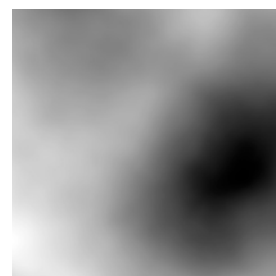
H=0.5



H=0.75

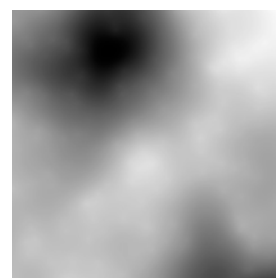
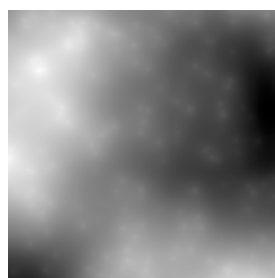
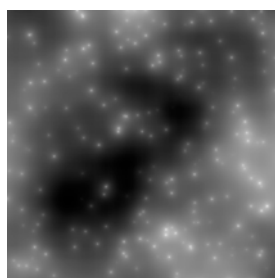
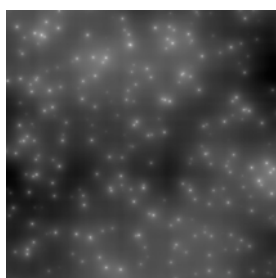


H=1.25



H=1.75

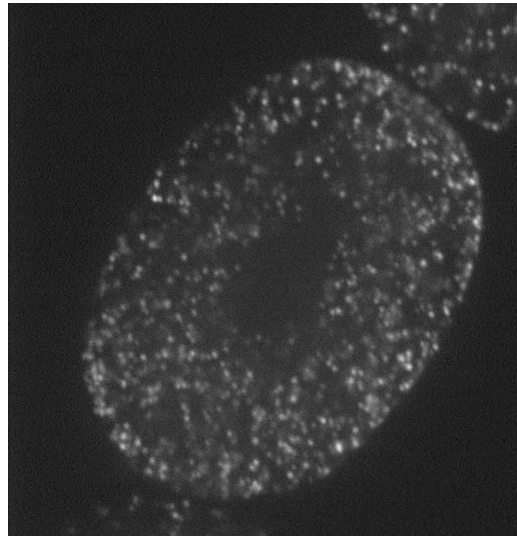
Sparse (generalized Poisson)



(U.-Tafti, *IEEE-SP* 2010)

20

Powers of ten: from astronomy to biology



21

RECONSTRUCTION OF BIOMEDICAL IMAGES

- Discretization of reconstruction problem
- Signal reconstruction algorithm (MAP)
- Examples of image reconstruction
 - Deconvolution microscopy
 - X-ray tomography
 - Cryo-electron tomography
 - Phase contrast tomography

22

Discretization of reconstruction problem

Spline-like reconstruction model: $s(\mathbf{r}) = \sum_{\mathbf{k} \in \Omega} s[\mathbf{k}] \beta_{\mathbf{k}}(\mathbf{r}) \iff \mathbf{s} = (s[\mathbf{k}])_{\mathbf{k} \in \Omega}$

■ Innovation model

$$\mathbf{L} \mathbf{s} = \mathbf{w}$$

$$\mathbf{s} = \mathbf{L}^{-1} \mathbf{w}$$

Discretization

$$\mathbf{u} = \mathbf{L} \mathbf{s} \quad (\text{matrix notation})$$

p_U is part of **infinitely divisible** family

■ Physical model: image formation and acquisition

$$y_m = \int_{\mathbb{R}^d} s_1(\mathbf{x}) \eta_m(\mathbf{x}) d\mathbf{x} + n[m] = \langle s_1, \eta_m \rangle + n[m], \quad (m = 1, \dots, M)$$

$$\mathbf{y} = \mathbf{y}_0 + \mathbf{n} = \mathbf{H} \mathbf{s} + \mathbf{n}$$

\mathbf{n} : i.i.d. noise with pdf p_N

$$[\mathbf{H}]_{m,\mathbf{k}} = \langle \eta_m, \beta_{\mathbf{k}} \rangle = \int_{\mathbb{R}^d} \eta_m(\mathbf{r}) \beta_{\mathbf{k}}(\mathbf{r}) d\mathbf{r}: \quad (M \times K) \text{ system matrix}$$

23

Posterior probability distribution

$$\begin{aligned} p_{S|Y}(\mathbf{s}|\mathbf{y}) &= \frac{p_{Y|S}(\mathbf{y}|\mathbf{s}) p_S(\mathbf{s})}{p_Y(\mathbf{y})} = \frac{p_N(\mathbf{y} - \mathbf{H}\mathbf{s}) p_S(\mathbf{s})}{p_Y(\mathbf{y})} && (\text{Bayes' rule}) \\ &= \frac{1}{Z} p_N(\mathbf{y} - \mathbf{H}\mathbf{s}) p_S(\mathbf{s}) \end{aligned}$$

$$\mathbf{u} = \mathbf{L} \mathbf{s} \quad \Rightarrow \quad p_S(\mathbf{s}) \propto p_U(\mathbf{L}\mathbf{s}) \approx \prod_{\mathbf{k} \in \Omega} p_U([\mathbf{L}\mathbf{s}]_{\mathbf{k}})$$

■ Additive white Gaussian noise scenario (AWGN)

$$p_{S|Y}(\mathbf{s}|\mathbf{y}) \propto \exp\left(-\frac{\|\mathbf{y} - \mathbf{H}\mathbf{s}\|^2}{2\sigma^2}\right) \prod_{\mathbf{k} \in \Omega} p_U([\mathbf{L}\mathbf{s}]_{\mathbf{k}})$$

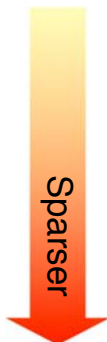
... and then take the log and maximize ...

24

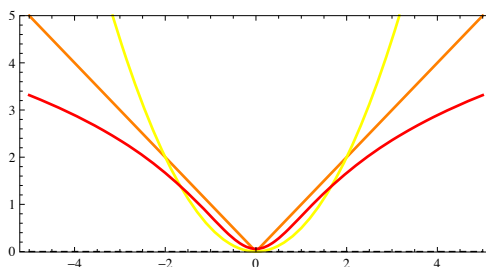
General form of MAP estimator

$$\mathbf{s}_{\text{MAP}} = \operatorname{argmin} \left(\frac{1}{2} \|\mathbf{y} - \mathbf{H}\mathbf{s}\|_2^2 + \sigma^2 \sum_n \Phi_U([\mathbf{L}\mathbf{s}]_n) \right)$$

- Gaussian: $p_U(x) = \frac{1}{\sqrt{2\pi}\sigma_0} e^{-x^2/(2\sigma_0^2)} \Rightarrow \Phi_U(x) = \frac{1}{2\sigma_0^2} x^2 + C_1$
- Laplace: $p_U(x) = \frac{\lambda}{2} e^{-\lambda|x|} \Rightarrow \Phi_U(x) = \lambda|x| + C_2$
- Student: $p_U(x) = \frac{1}{B(r, \frac{1}{2})} \left(\frac{1}{x^2 + 1} \right)^{r+\frac{1}{2}} \Rightarrow \Phi_U(x) = (r + \frac{1}{2}) \log(1 + x^2) + C_3$



Potential: $\Phi_U(x) = -\log p_U(x)$

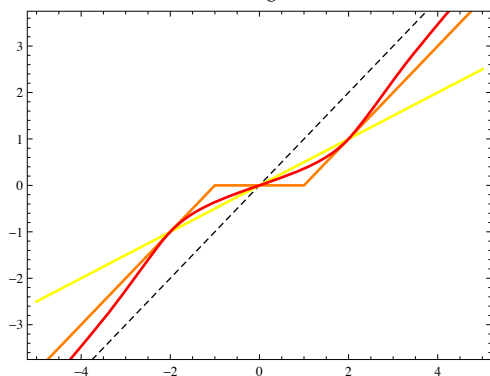


25

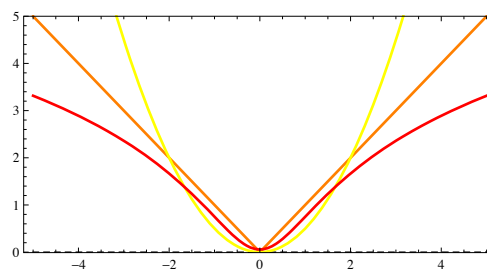
Proximal operator: pointwise denoiser

$$\operatorname{prox}_{\Phi_U}(y; \sigma^2) = \operatorname{argmin}_{u \in \mathbb{R}} \frac{1}{2} |y - u|^2 + \sigma^2 \Phi_U(u)$$

$$\tilde{u} = \operatorname{prox}_{\Phi_U}(y; 1)$$



$\sigma^2 \Phi_U(u)$



- linear attenuation ℓ_2 minimization
- soft-threshold ℓ_1 minimization
- shrinkage function $\approx \ell_p$ relaxation for $p \rightarrow 0$

26

Maximum a posteriori (MAP) estimation

■ Constrained optimization formulation

Auxiliary **innovation** variable: $\mathbf{u} = \mathbf{L}\mathbf{s}$

$$\mathbf{s}_{\text{MAP}} = \arg \min_{\mathbf{s} \in \mathbb{R}^K} \left(\frac{1}{2} \|\mathbf{y} - \mathbf{H}\mathbf{s}\|_2^2 + \sigma^2 \sum_n \Phi_U([\mathbf{u}]_n) \right) \text{ subject to } \mathbf{u} = \mathbf{L}\mathbf{s}$$

■ Augmented Lagrangian method

Quadratic penalty term: $\frac{\mu}{2} \|\mathbf{L}\mathbf{s} - \mathbf{u}\|_2^2$

Lagrange multiplier vector: $\boldsymbol{\alpha}$

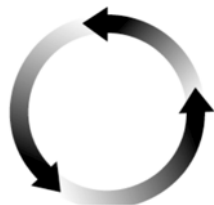
$$\mathcal{L}_{\mathcal{A}}(\mathbf{s}, \mathbf{u}, \boldsymbol{\alpha}) = \frac{1}{2} \|\mathbf{g} - \mathbf{H}\mathbf{s}\|_2^2 + \sigma^2 \sum_n \Phi_U([\mathbf{u}]_n) + \boldsymbol{\alpha}^T (\mathbf{L}\mathbf{s} - \mathbf{u}) + \frac{\mu}{2} \|\mathbf{L}\mathbf{s} - \mathbf{u}\|_2^2$$

27

Alternating direction method of multipliers (ADMM)

$$\mathcal{L}_{\mathcal{A}}(\mathbf{s}, \mathbf{u}, \boldsymbol{\alpha}) = \frac{1}{2} \|\mathbf{g} - \mathbf{H}\mathbf{s}\|_2^2 + \sigma^2 \sum_n \Phi_U([\mathbf{u}]_n) + \boldsymbol{\alpha}^T (\mathbf{L}\mathbf{s} - \mathbf{u}) + \frac{\mu}{2} \|\mathbf{L}\mathbf{s} - \mathbf{u}\|_2^2$$

Sequential minimization



$$\mathbf{s}^{k+1} \leftarrow \arg \min_{\mathbf{s} \in \mathbb{R}^N} \mathcal{L}_{\mathcal{A}}(\mathbf{s}, \mathbf{u}^k, \boldsymbol{\alpha}^k)$$

$$\boldsymbol{\alpha}^{k+1} = \boldsymbol{\alpha}^k + \mu (\mathbf{L}\mathbf{s}^{k+1} - \mathbf{u}^k)$$

$$\mathbf{u}^{k+1} \leftarrow \arg \min_{\mathbf{u} \in \mathbb{R}^N} \mathcal{L}_{\mathcal{A}}(\mathbf{s}^{k+1}, \mathbf{u}, \boldsymbol{\alpha}^{k+1})$$

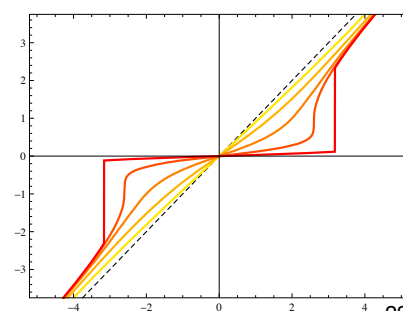
Linear inverse problem: $\mathbf{s}^{k+1} = (\mathbf{H}^T \mathbf{H} + \mu \mathbf{L}^T \mathbf{L})^{-1} (\mathbf{H}^T \mathbf{y} + \mathbf{z}^{k+1})$

with $\mathbf{z}^{k+1} = \mathbf{L}^T (\mu \mathbf{u}^k - \boldsymbol{\alpha}^k)$

Nonlinear denoising: $\mathbf{u}^{k+1} = \text{prox}_{\Phi_U}(\mathbf{L}\mathbf{s}^{k+1} + \frac{1}{\mu} \boldsymbol{\alpha}^{k+1}; \frac{\sigma^2}{\mu})$

■ Proximal operator tailored to stochastic model

$$\text{prox}_{\Phi_U}(y; \lambda) = \arg \min_u \frac{1}{2} |y - u|^2 + \lambda \Phi_U(u)$$



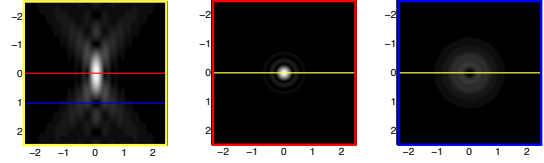
Cauchy prior with increasing s_0

28

Deconvolution of fluorescence micrographs

Physical model of a diffraction-limited microscope

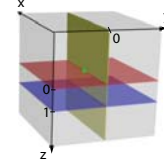
$$g(x, y, z) = (h_{3D} * s)(x, y, z)$$



3-D point spread function (PSF)

$$h_{3D}(x, y, z) = I_0 \left| p_\lambda \left(\frac{x}{M}, \frac{y}{M}, \frac{z}{M^2} \right) \right|^2$$

$$p_\lambda(x, y, z) = \int_{\mathbb{R}^2} P(\omega_1, \omega_2) \exp\left(j2\pi z \frac{\omega_1^2 + \omega_2^2}{2\lambda f_0^2}\right) \exp\left(-j2\pi \frac{x\omega_1 + y\omega_2}{\lambda f_0}\right) d\omega_1 d\omega_2$$



Optical parameters

- λ : wavelength (emission)
- M : magnification factor
- f_0 : focal length
- $P(\omega_1, \omega_2) = \mathbb{1}_{\|\omega\| < R_0}$: pupil function
- $\text{NA} = n \sin \theta = R_0 / f_0$: numerical aperture

29

Deconvolution: numerical set-up

Discretization

$\omega_0 \leq \pi$ and representation in (separable) sinc basis $\{\text{sinc}(\mathbf{x} - \mathbf{k})\}_{\mathbf{k} \in \mathbb{Z}^d}$

Analysis functions: $\eta_{\mathbf{m}}(x, y, z) = h_{3D}(x - m_1, y - m_2, z - m_3)$

$$\begin{aligned} [\mathbf{H}]_{\mathbf{m}, \mathbf{k}} &= \langle \eta_{\mathbf{m}}, \text{sinc}(\cdot - \mathbf{k}) \rangle \\ &= \langle h_{3D}(\cdot - \mathbf{m}), \text{sinc}(\cdot - \mathbf{k}) \rangle \\ &= (\text{sinc} * h_{3D})(\mathbf{m} - \mathbf{k}) = h_{3D}(\mathbf{m} - \mathbf{k}). \end{aligned}$$

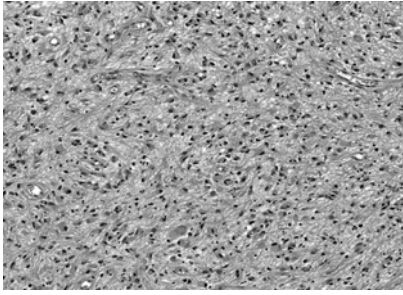
\mathbf{H} and \mathbf{L} : convolution matrices diagonalized by discrete Fourier transform

Linear step of ADMM algorithm implemented using the FFT

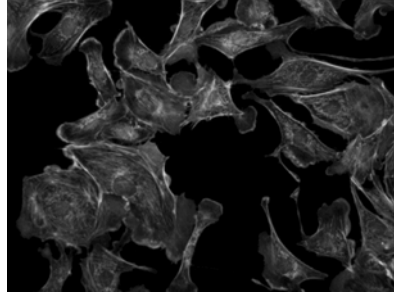
$$\begin{aligned} \mathbf{s}^{k+1} &= (\mathbf{H}^T \mathbf{H} + \mu \mathbf{L}^T \mathbf{L})^{-1} (\mathbf{H}^T \mathbf{y} + \mathbf{z}^{k+1}) \\ \text{with } \mathbf{z}^{k+1} &= \mathbf{L}^T (\mu \mathbf{u}^k - \boldsymbol{\alpha}^k) \end{aligned}$$

30

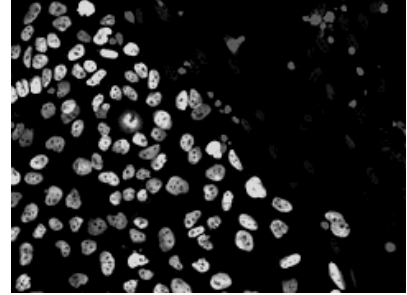
2D deconvolution experiment



Astrocytes cells



bovine pulmonary artery cells



human embryonic stem cells

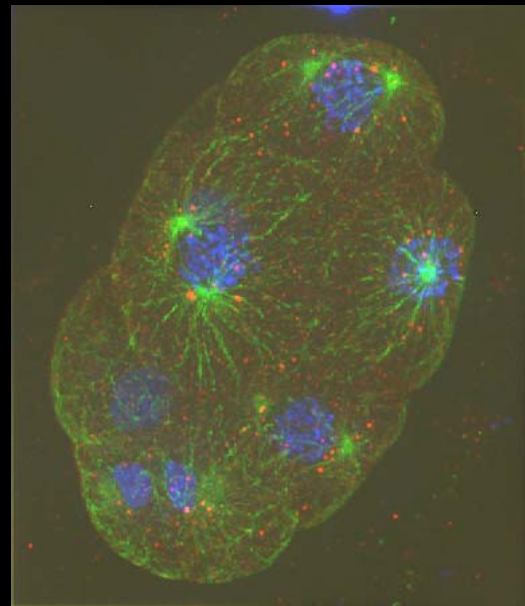
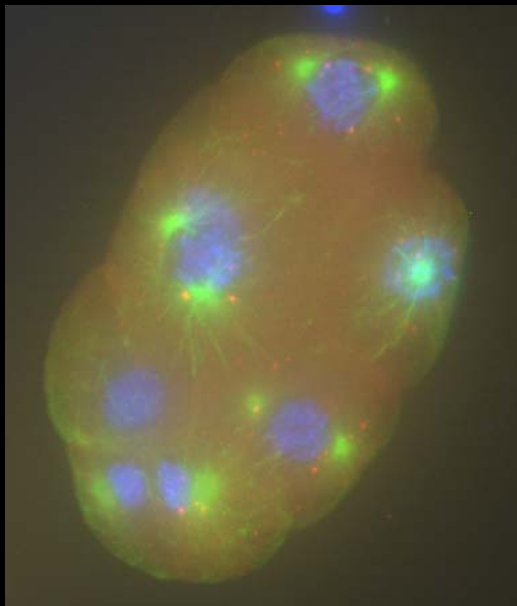
L : gradient

Deconvolution results in dB

Optimized parameters

	Gaussian Estimator	Laplace Estimator	Student's Estimator
Astrocytes cells	12.18	10.48	10.52
Pulmonary cells	16.90	19.04	18.34
Stem cells	15.81	20.19	20.50

3D deconvolution with sparsity constraints



Maximum intensity projections of $384 \times 448 \times 260$ image stacks;

Leica DM 5500 widefield epifluorescence microscope with a $63 \times$ oil-immersion objective;

C. Elegans embryo labeled with Hoechst, Alexa488, Alexa568;

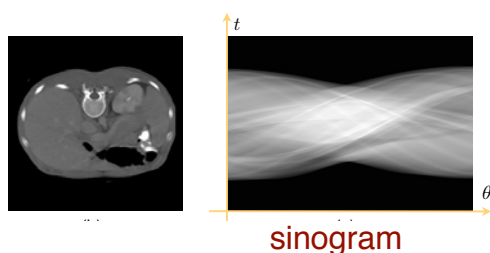
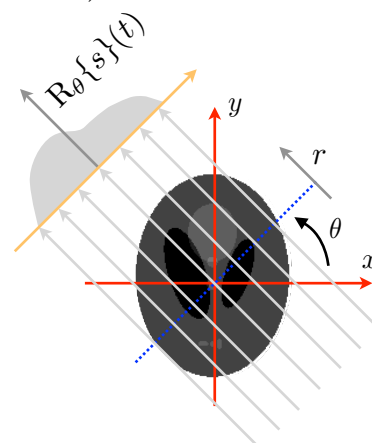
(Vonesch-U. *IEEE Trans. Im. Proc.* 2009)

Computed tomography (straight rays)

Projection geometry: $\mathbf{x} = t\boldsymbol{\theta} + r\boldsymbol{\theta}^\perp$ with $\boldsymbol{\theta} = (\cos \theta, \sin \theta)$

Radon transform (line integrals)

$$\begin{aligned} R_\theta\{s(\mathbf{x})\}(t) &= \int_{\mathbb{R}} s(t\boldsymbol{\theta} + r\boldsymbol{\theta}^\perp) dr \\ &= \int_{\mathbb{R}^2} s(\mathbf{x})\delta(t - \langle \mathbf{x}, \boldsymbol{\theta} \rangle) d\mathbf{x} \end{aligned}$$



Equivalent analysis functions: $\eta_m(\mathbf{x}) = \delta(t_m - \langle \mathbf{x}, \boldsymbol{\theta}_m \rangle)$

Computed tomography reconstruction results

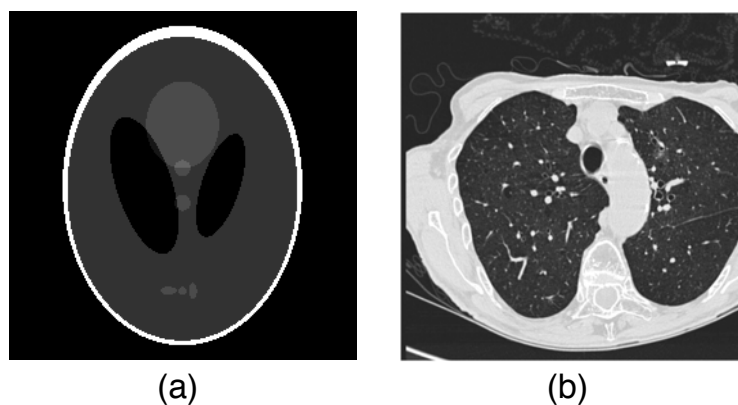


Figure 10.6 Images used in X-ray tomographic reconstruction experiments. (a) The Shepp-Logan (SL) phantom. (b) Cross section of a human lung.

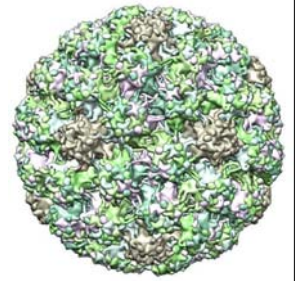
Table 10.4 Reconstruction results of X-ray computed tomography using different estimators.

	Directions	Estimation performance (SNR in dB)		
		Gaussian	Laplace	Student's
SL Phantom	120	16.8	17.53	18.76
SL Phantom	180	18.13	18.75	20.34
Lung	180	22.49	21.52	21.45
Lung	360	24.38	22.47	22.37

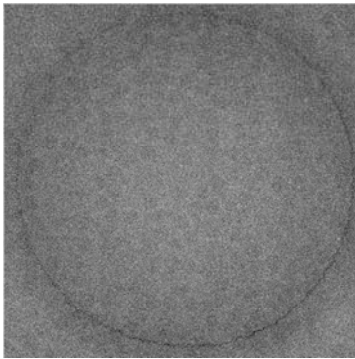
L: discrete gradient

EM: Single particle analysis

Bovine papillomavirus



Cryo-electron micrograph



Number of pixels: $256 \times 256 \times 256$

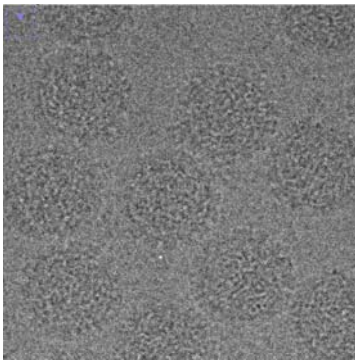
Resolution: 2.474 Å

Number of particles: 800

Type of symmetry: $i\bar{h}$ (60 fold symmetry)



C.-O. Sorzano



noisy projection of identical particles, with unknown orientations

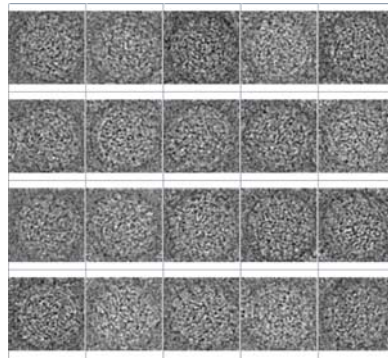
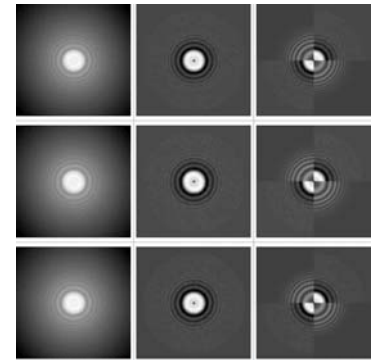


image alignment and classification

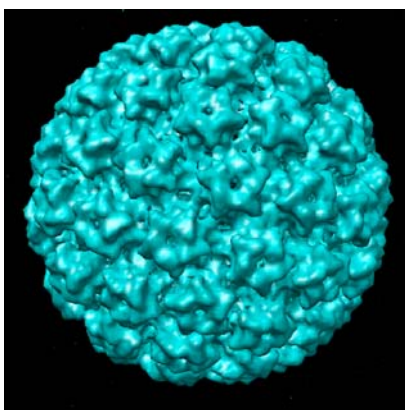


CTF estimation and correction

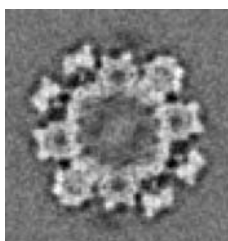
Image reconstruction (real data)



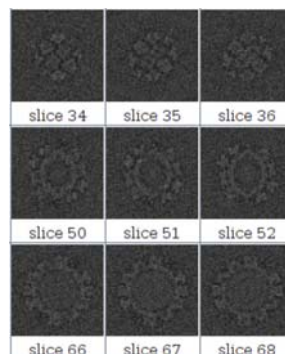
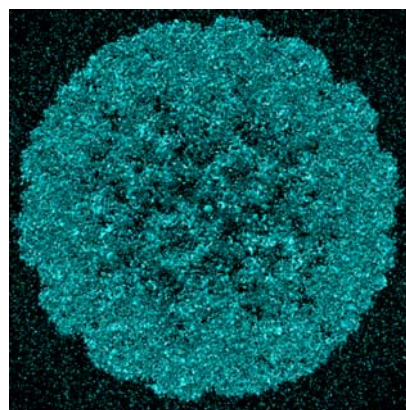
Standard Fourier-based reconstruction



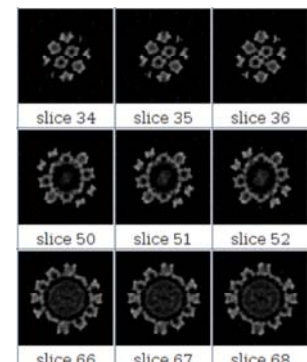
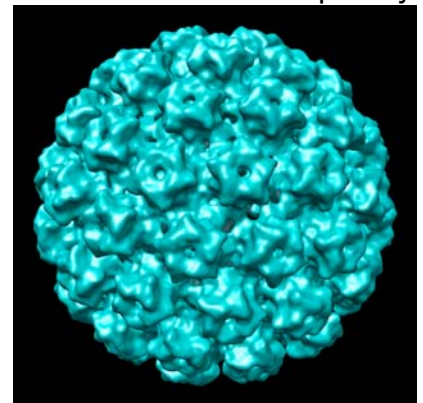
6.185 Å

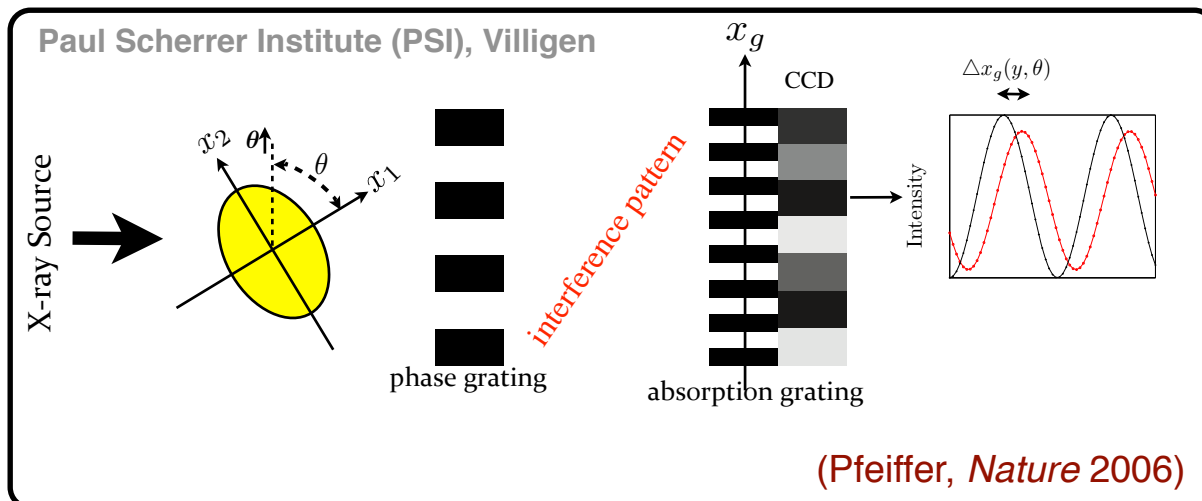


High-resolution Fourier-based reconstruction



High-resolution reconstruction with sparsity





Mathematical model

$$g(t, \theta) = \frac{\partial}{\partial t} R_{\theta} \{f\}(t)$$



$$\mathbf{g} = \mathbf{H} \mathbf{s}$$

$$[\mathbf{H}]_{(i,j),\mathbf{k}} = \frac{\partial}{\partial t} P_{\theta_j} \beta_{\mathbf{k}}(t_j)$$

37

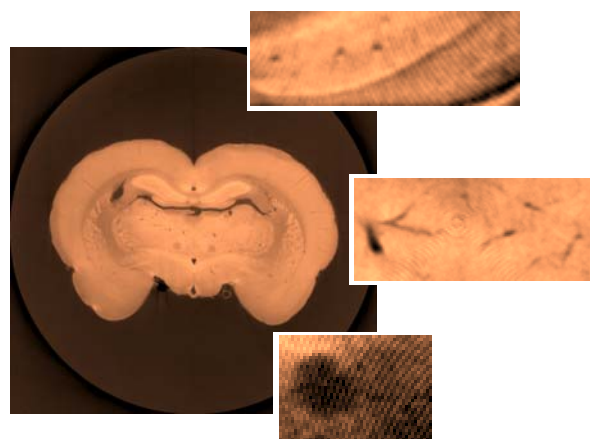
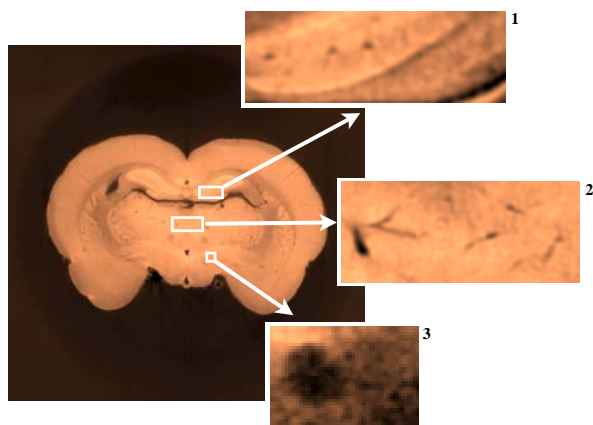
Experimental results

Rat brain reconstruction with 721 projections

ADMM-PCG (TV)

FBP

(Pfeiffer et al. *Nucl. Inst. Meth. Phys. Res.* 2007)



\mathbf{L} : discrete gradient, $\Phi(u) = \lambda|u|$

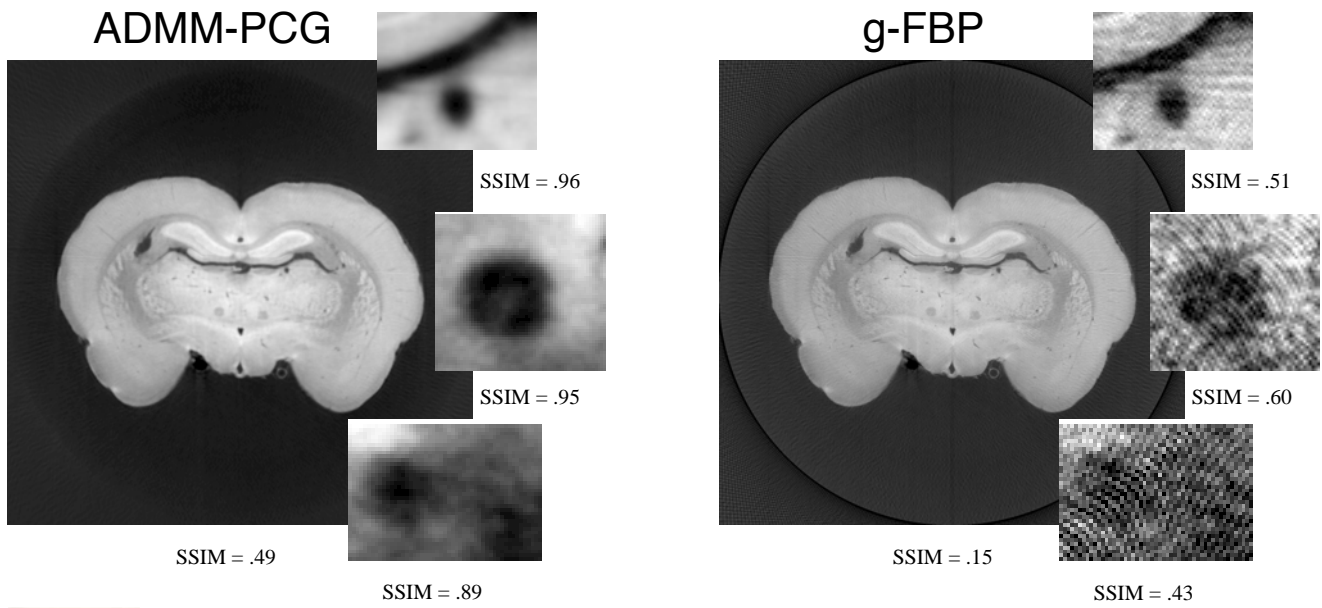
Collaboration: Prof. Marco Stampanoni, TOMCAT PSI / ETHZ

38

Reducing the numbers of views



Rat brain reconstruction with 181 projections

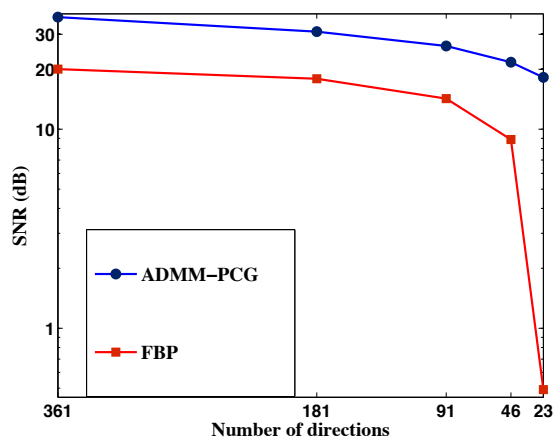


Collaboration: Prof. Marco Stampanoni, TOMCAT PSI / ETHZ

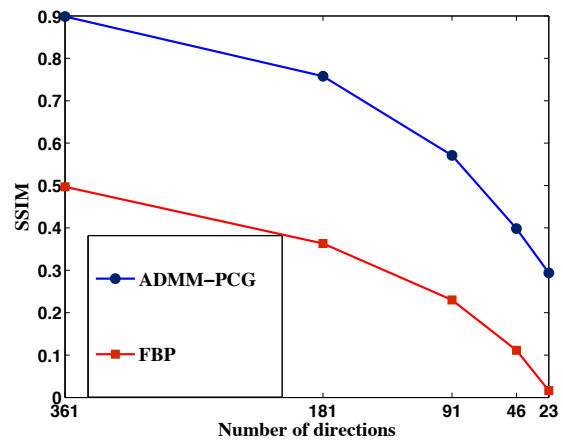
(Nichian et al. *Optics Express* 2013)

Performance evaluation

Goldstandard: high-quality iterative reconstruction with 721 views



(a)



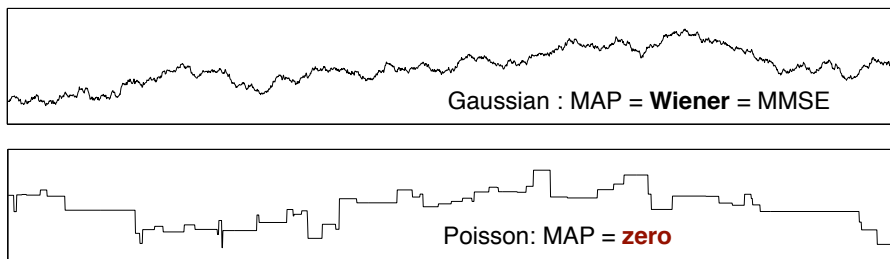
(b)

⇒ Reduction of acquisition time by a factor 10 (or more) ?

CAN WE GO BEYOND MAP ESTIMATION ?

⇒ A detailed investigation of simpler denoising problem

Test case: Lévy processes



1. Can we compute the “best”= MMSE estimator ?

Yes, by using **belief propagation** (Kamilov et al., *IEEE-SP* 2013)

2. Can we compute it with an iterative MAP-type algorithm ?

Yes (with the help of **Haar wavelets**) by optimizing the **thresholding function**

41

Pointwise MMSE estimators for AWGN

■ Minimum-mean-square-error (MMSE) estimator from $y = x + n$

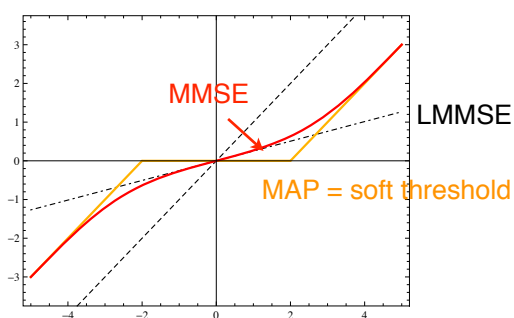
$$x_{\text{MMSE}}(y) = \mathbb{E}\{X|Y = y\} = \int_{\mathbb{R}} x \cdot p_{X|Y}(x|y) dx$$

AWGN probability model $\implies p_{Y|X}(y|x) = g_{\sigma}(y - x)$ and $p_Y = g_{\sigma} * p_X$

g_{σ} : Gaussian pdf (zero mean with variance σ^2)

■ Stein's formula for AWGN

$$x_{\text{MMSE}}(y) = y - \sigma^2 \Phi'_Y(y) \quad \text{where} \quad \Phi'_Y(y) = -\frac{d}{dy} \log p_Y(y) = -\frac{p'_Y(y)}{p_Y(y)}$$



Laplacian

42

Iterative wavelet-based denoising: MAP → MMSE

Consistent Cycle Spinning (CCS)

(Kamilov, IEEE-SPL 2012)

CCS denoising: Solves $\min_{\mathbf{s}} \left\{ \frac{1}{2} \|\mathbf{s} - \mathbf{y}\|_2^2 + \frac{\tau}{M} \Phi(\mathbf{A}\mathbf{s}) \right\}$ where \mathbf{A} is a tight frame

input: $\mathbf{y}, \mathbf{s}^0 \in \mathbb{R}^N, \tau, \mu \in \mathbb{R}^+$

set: $k = 0, \boldsymbol{\lambda}^0 = \mathbf{0}, \mathbf{u} = \mathbf{A}\mathbf{y};$

repeat

$$\mathbf{z}^{k+1} = \text{prox}_{\Phi} \left(\frac{1}{1+\mu} (\mathbf{u} + \mu \mathbf{A}\mathbf{s}^k + \boldsymbol{\lambda}^k); \frac{\tau}{1+\mu} \right)$$

$$\text{or } \mathbf{z}^{k+1} = v_{\text{MMSE}} \left(\tilde{\mathbf{z}}^{k+1}; \frac{\sigma^2}{1+\mu} \right)$$

$$\mathbf{s}^{k+1} = \mathbf{A}^\dagger \left(\mathbf{z}^{k+1} - \frac{1}{\mu} \boldsymbol{\lambda}^k \right)$$

$$\boldsymbol{\lambda}^{k+1} = \boldsymbol{\lambda}^k - \mu (\mathbf{z}^{k+1} - \mathbf{A}\mathbf{s}^{k+1})$$

$$k = k + 1$$

until stopping criterion

return $\mathbf{s} = \mathbf{s}^k$

- CCS constraint: $\mathbf{z} = \mathbf{A}\mathbf{s}$ with $\|\mathbf{z}\|^2 = M\|\mathbf{s}\|^2$ (enforces energy conservation)

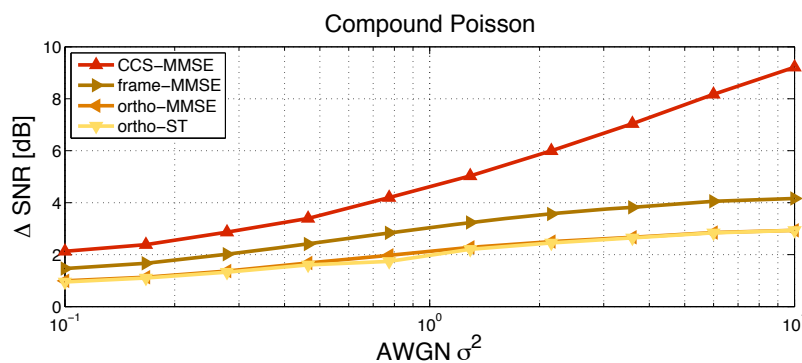
- Variation on a theme: substitute MAP shrinkage by **MMSE shrinkage**

(Kazerouni, IEEE-SPL 2013)

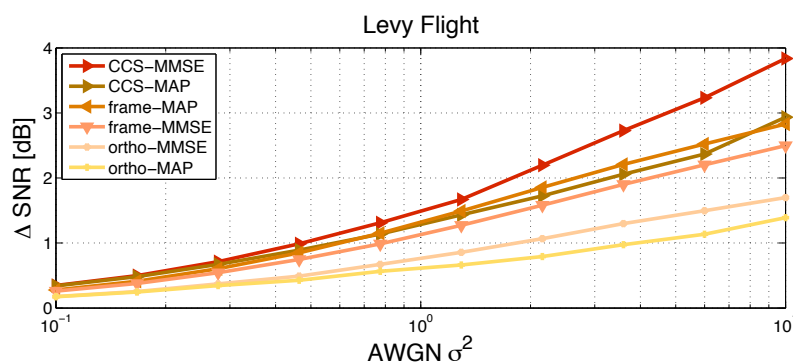
⇒ Iterative MMSE denoising

43

Comparison of wavelet denoising strategies



Key empirical finding: CCS MMSE denoising yields optimal solution !!!!



CONCLUSION

- Unifying continuous-domain stochastic model
 - Backward compatibility with classical Gaussian theory
 - Operator-based formulation: Lévy-driven SDEs or SPDEs
 - **Gaussian** vs. **sparse** (generalized Poisson, student, $S\alpha S$)
- Regularization
 - Sparsification via “operator-like” behavior (whitening)
 - Specific family of id potential functions (typ., non-convex)
- Conceptual framework for sparse signal recovery
 - Principled approach for the development of novel algorithms
 - Challenge: algorithms for solving large-scale problems in imaging:
Cryo-electron tomography, diffraction tomography, dynamic MRI (3D + time), etc...
 - **Beyond MAP reconstruction: MMSE with learning (self-tuning)**

45

Conclusion (Cont'd)

The continuous-domain theory of sparse stochastic processes is compatible with both

20th century SP = **linear and Fourier-based algorithms**, and

21st century SP = **non-linear, sparsity-promoting, wavelet-based algorithms**

... but there are still many open questions ...

46

References

■ Theory of sparse stochastic processes

- M. Unser and P. Tafti, ***An Introduction to Sparse Stochastic Processes***, Cambridge University Press, 2014; preprint, available at <http://www.sparseprocesses.org>.
- M. Unser, P.D. Tafti, "Stochastic models for sparse and piecewise-smooth signals", *IEEE Trans. Signal Processing*, vol. 59, no. 3, pp. 989-1006, March 2011.
- M. Unser, P. Tafti, and Q. Sun, "A unified formulation of Gaussian vs. sparse stochastic processes—Part I: Continuous-domain theory," *IEEE Trans. Information Theory*, vol. 60, no. 3, pp. 1945-1962, March 2014.

■ Algorithms and imaging applications

- E. Bostan, U.S. Kamilov, M. Nilchian, M. Unser, "Sparse Stochastic Processes and Discretization of Linear Inverse Problems," *IEEE Trans. Image Processing*, vol. 22, no. 7, pp. 2699-2710, 2013.
- C. Vonesch, M. Unser, "A Fast Multilevel Algorithm for Wavelet-Regularized Image Restoration," *IEEE Trans. Image Processing*, vol. 18, no. 3, pp. 509-523, March 2009.
- M. Nilchian, C. Vonesch, S. Lefkimmiatis, P. Modregger, M. Stampanoni, M. Unser, "Constrained Regularized Reconstruction of X-Ray-DPCI Tomograms with Weighted-Norm," *Optics Express*, vol. 21, no. 26, pp. 32340-32348, 2013.
- A. Entezari, M. Nilchian, M. Unser, "A Box Spline Calculus for the Discretization of Computed Tomography Reconstruction Problems," *IEEE Trans. Medical Imaging*, vol. 31, no. 8, pp. 1532-1541, 2012.

47

Acknowledgments

Many thanks to

- Dr. Pouya Tafti
- Prof. Qiyu Sun
- Prof. Arash Amini
- Dr. Cédric Vonesch
- Dr. Matthieu Guerquin-Kern
- Emrah Bostan
- Ulugbek Kamilov
- Masih Nilchian



■ Members of EPFL's Biomedical Imaging Group



- Preprints and demos: <http://bigwww.epfl.ch/>

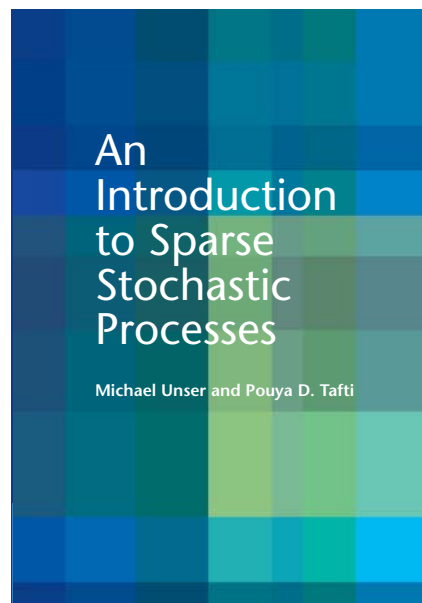
48

ebook: web preprint



Chapter by chapter

- ▶ [Cover](#)
- ▶ [Introduction](#)
- ▶ [Road map to the monograph](#)
- ▶ [Mathematical context and background](#)
- ▶ [Continuous-domain innovation models](#)
- ▶ [Operators and their inverses](#)
- ▶ [Splines and wavelets](#)
- ▶ [Sparse stochastic processes](#)
- ▶ [Sparse representations](#)
- ▶ [Infinite divisibility and transform-domain statistics](#)
- ▶ [Sparse signal recovery](#)
- ▶ [Wavelet-domain methods](#)



Cover design: Annette Unser

<http://www.sparseprocesses.org>